HPC Software for Massively Parallel Simulation of 3D Electromagnetic Nano-structures

A. Al-Jarro[1], C. G. Biris[1,2], and N. C. Panoiu[1]

[1]*Department of Electronic and Electrical Engineering, University College London, Torrington Place, London WC1E 7JE, United Kingdom*

[2]*High Performance Computing Center, West University of Timisoara, B-dul Vasile Parvan, Nr. 4, Timisoara 300223, Timis, Romania*

Abstract

Advanced research in photonic materials has shown that rapid breakthroughs in device applications go hand-in-hand with the development of efficient, computationally powerful software tools. Thus, high fabrication costs of complex photonic nano-structures and devices make it imperative to have access to computational tools based on efficient algorithms, which can greatly reduce the design-fabrication-testing cycle. In this context, computational techniques based on the multiple-scattering formalism have become a primary means to model a variety of scientific and engineering problems related to the electromagnetic wave interaction with arbitrary distributions of particles and materials. In this work, we have extended ***OPTIMET*** (OPTIcal METa-materials) code, which is based on the 2D multiple scattering matrix method, to allow for the analysis of electromagnetic wave interaction with large ensembles of 3D micro- and nano-particles that are periodically or arbitrarily distributed in an otherwise homogeneous background. The newly developed software, ***OPTIMET-3D***, has the following additional functionalities, which dramatically enhance its computational capabilities: (i) The extension of the code capability to 3D photonic structures, (ii) The capability to model non-linear (second-order) optical respons of ensembles of particles, (iii) The capability to describe efficiently periodically distributed electromagnetic scatterers, (iv) The design and development of the software so as to render it suitable to run efficiently on parallel HPC systems.

Table of Contents

1. Introduction

Over the past few years we have witnessed tremendous progress in the design of photonic nano-materials, nano-devices and circuits, which in part has been greatly accelerated by the availability of user-friendly, computationally powerful software tools for device simulation and design. Advanced research in integrated optics and photonics has shown that rapid, informed advances in photonic device applications go hand-in-hand with the development of highly efficient computational simulation tools. Thus, high fabrication costs of complex photonic nano-devices make it imperative to have access to computational tools based on efficient algorithms, which can greatly accelerate the device design process and reduce the design-fabrication-testing cycle. *The future photonic computational tools should be able to model a distributed multifunctional device "continuum" in which the light is generated, processed and collected in the same physical space*. This complexity of the architecture of photonics circuitry implies that future computational tools must fully integrate the description of physical phenomena that take place over multiple temporal, spectral and spatial scales. It is therefore evident that in order to achieve rapid advances in nano-photonics, research in computational methods and development of new and versatile HPC codes are of crucial importance.

In recent years, computational techniques based on the multiple-scattering formalism have become a primary means for modelling a variety of scientific and engineering problems related to the electromagnetic wave interaction with systems of particles and material media [1-5]. Thus, computational methods based on the multiple-scattering matrix (MSM) algorithm, also called the *T*-matrix method, play a central role in modelling a vast array of applications, such as photonic and plasmonic crystals (transmission, reflection, absorption, density of states), metamaterials, nano-photonics (nano-lasers, plasmonic materials), radar signature technology, wireless communications devices, antennae, microwave devices, bio-photonics and biomedical imaging/treatment. The versatility of the MSM method allows one to study the electromagnetic waves interaction with distributions of scatterers under a broad set of boundary conditions, material parameters and geometries (periodic and non-periodic boundary conditions, 2D and 3D geometries, in the time and frequency domains) and can be applied to scattering systems that contain both linear and non-linear media. *More importantly, there is a scarcity of HPC codes currently available on HECToR for electromagnetic simulations* (in fact, at the time of writing this report we were aware of no such code). Similarly, on *Legion* (Legion@UCL, UCL's HPC compute platform and the *HPC system on which the code developed as part of this project is intended to be used*) there is only one HPC electromagnetic simulator (MEEP), a time domain solver based on the FDTD method.

2. Project Objectives

A versatile HPC tool for simulation of photonic materials must provide two major capabilities: First, it should describe various geometries, which can be 2D or 3D periodically or randomly arranged objects, a large variety of basic building blocks of photonic materials and should provide a full characterisation of the properties of the material both in the time and frequency domains. Second, the HPC software should be efficient and easy to use so as to appeal to a large user base. To this end, *the main aim of this project was to develop a versatile, easy to use HPC software for massively parallel simulation both in the time and frequency domains of 2D and 3D materials that are periodically or randomly structured*. The proposed software development work has been organised along three major work packages:

Work package 1: Extension of OPTIMET to 3D structures

This part of the project was devoted to the extension of the current OPTIMET code [5] to 3D geometry.

- Incorporate in the code vector spherical wave functions (VSWF) *via* the addition of spherical harmonic functions;
- Implement the functions that construct the scattering matrix of the system and the 3D fields. The scattering matrix of the system is constructed at node level whilst the spectral and time domain calculations are implemented *via* MPI and distributed across the available nodes.
- Implement the functions that compute the system cross-sections. This task amounted to writing the routines for calculating the total, scattering and absorption cross-sections of the system.

Work package 2: Implementation of periodic boundary conditions

In this part of the project the periodic boundary conditions capability was added to the code.

- Implement the routines to compute the transmission/reflection matrices.
- Implement the functions for the transmission/reflection matrices of a set of layers of scatterers.
- Implement the routines that compute the transmission and reflection coefficients of a material slab.

Work package 3: Extension of OPTIMET so as to incorporate quadratic nonlinearities
OPTIMET-3D was developed to incorporate the effects induced by quadratic optical nonlinearities.

- Write a set of routines for computing the nonlinear scattering matrix of the system.
- Write the functions that compute the total, scattering and absorption cross-sections of the system.

We want to mention here that originally we intended to implement the simpler case, namely, that of *cubic (Kerr) optical nonlinearity*. However, as the project progressed, it became clear that we would be able to develop a branch of the code for modelling the much more complex case (and more important from a practical point of view), that of *quadratically non-linear optical interactions*. The main reason for this change in strategy was that the developer of the original version of the code, Dr Claudiu Biris, was able to invest in this project more time than it has been originally anticipated.

3. Project Outcomes

The main outcomes of the project can be divided in two main categories, namely, a versatile HPC software (OPTIMET-3D) that can accurately model the interaction between electromagnetic waves and arbitrary distributions of metallic, dielectric and semiconductor particles, and an enhanced capability to investigate and solve a multitude of scientific problems that are relevant to several areas of science and technology, including optoelectronics, photonics, materials science, plasmonics, nanotechnology, non-linear optics and surface science. In fact, we have already used OPTIMET-3D to demonstrate for the first time that, surprisingly, super-chiral light can be generated in clusters of silicon nano-spheres; a conference paper on this topic will be presented shortly after the completion of the project [6].

OPTIMET-3D has been developed to be used on *Legion* (Legion@UCL) UCL's HPC cluster. *Legion* comprises 904 nodes offering over 5600 processor cores, each with between 2GB and 4GB RAM. Most of the system is connected by high-performance interconnect. The cluster is coupled to a large-scale high-performance file system, with a total capacity of 192 TB. The cluster features a range of best-in-class compilers and related tools for serial and parallel code development, such as Intel C++ and FORTRAN compilers, Pathscale Compiler Suite, a broad set of libraries, such as Intel's Math Kernel Library (MKL), BLACS, LAPACK and ScaLAPACK, and software tools for development of parallel code, such as MPICH2 and OpenMP. The service is currently further expanded, with new compute capacity being added to the cluster. The current version of OPTIMET-3D deployed on *Legion* was built using Intel's Compiler Collection version 11.1 and uses the OpenMPI 1.4.1 parallel library suite.

OPTIMET-3D has also been successfully ported and run on two other HPC platforms, specifically, the InfraGrid and BlueGene/P clusters at the West University of Timisoara (Romania). InfraGrid is an Intel® Xeon cluster with 100 Quad Core CPUs clocked at 2.0 GHz. Each CPU has direct access to 10 GB of RAM and all share a 145 GB SAS local storage device. The system uses 40Gbps 4xQDR Infinipath interconnect to ensure fast and stable inter-node communications. OPTIMET-3D was deployed on InfraGrid using Intel's Compiler Collection version 11.1 and uses Intel's MPI 4.1 library. The second HPC platform is a BlueGene/P rack with 1024 Quad Core PowerPC-450 processors. Each CPU has access to 4GB of RAM and the cluster is connected to a 48×320 GB SAS IBM DS3524 networked storage arrays. Interconnect is provided by a Torus 3D network. To date, OPTIMET-3D has been tested on the BlueGene/P cluster but no production code has been run. These tests have been performed to ensure compatibility with IBM technologies, specifically, MKL was replaced by IBM's Engineering and Scientific Subroutine Library (ESSL) and the code was compiled with IBM's XL Compiler Suite, version 9.0, and linked with the IBM MPIx parallel library.

After full testing, OPTIMET-3D will be hosted at http://www.ee.ucl.ac.uk/~npanoiu/Software.html, on Dr Panoiu's webpage at UCL, and will be freely available for download. The software will also be made freely available to all interested users of *Legion*. In order to increase the dissemination and potential use of the software, we are also preparing a journal article that will be submitted together with the code to *Comp. Phys. Comm*. journal. OPTIMET-3D is currently stored on *BitBucket* in a Mercurial repository (https://bitbucket.org/cbiris/optimet3d). Access to it is available through any compatible Mercurial client that can access Mercurial repositories of version 1.4 or higher, such as "hg" for Unix or Tortoise HG for Windows. The current version of OPTIMET-3D has about 20500 lines of code. We use the following four branches, for development and code release:

- *default* – this is the default branch, which contains the current release version of OPTIMET-3D and also incorporates the previous software, OPTIMET. This branch would be accessed by users who are interested in using OPTIMET-3D, but do not wish to develop code using the API.

- *devel* – this is the main development branch for the serial version of the code. This version contains all the latest features of the code, as they are first tested in the serial version before being pushed onto the parallel development branch.
- *devel-parallel* – this is the main development branch for the parallel version of the code. This branch is a mirror of the *devel* branch but contains parallel version of the needed functions and classes. Since features are tested in the serial version first, this branch may occasionally have less features than the *devel* branch.
- *forward* – this is a private branch which is used only by the OPTIMET-3D developers to implement and perform initial tests of new features in future release versions of the code. Understandably, some of the features in this branch may be unstable or untested, so users who want to use OPTIMET-3D API should synchronise with the *devel* or *devel-parallel* branches.

The software tool developed as part of this project has three major capabilities, which have been implemented as part of the three major thrusts (work packages) of the software development work. The corresponding blocks of the code that implement these main features are parallelised. All parts of the source code are integrated in a single software tool, which makes it particularly easy to use and disseminate the code and to further develop it as well.

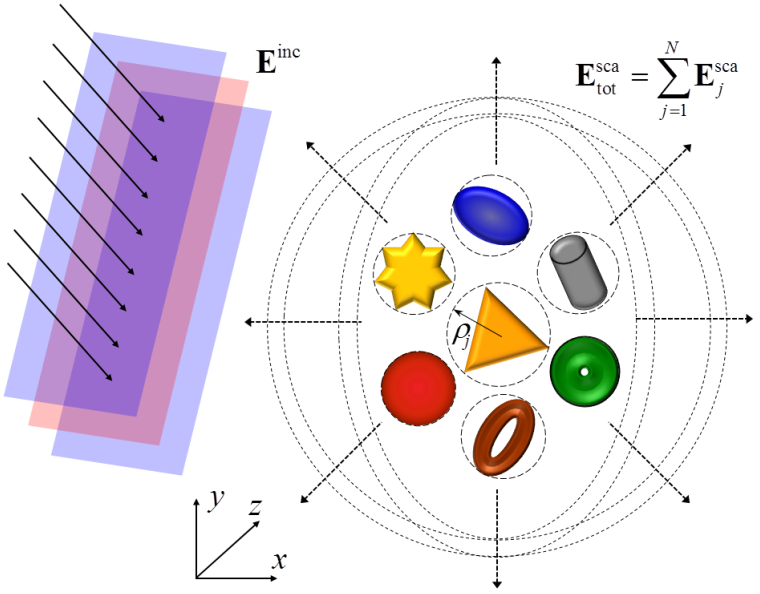

***Figure 1**. Schematic representation of the incident field/scattered field theoretical model and 3D structure of a cluster of arbitrary scatterers.*

First, unlike the previous version (OPTIMET), the HPC code can now model fully 3D electromagnetic structures (as schematically shown in Fig. 1). This represents a dramatic improvement of the code, particularly from a practical point of view. The electromagnetic scatterers can have rather arbitrary shape, including spheres, ellipsoids and pyramids. Additional shapes can be modelled by simply providing the parametric representation of the corresponding surface of the scatterer. Moreover, the scatterers can have different size, can be arbitrarily distributed and can consist of materials with different electromagnetic properties, provided *via* the electrical permittivity (ε) and magnetic permeability (μ). Once the configuration of the incoming field (direction and polarisation) and distribution of scatterers are provided, OPTIMET-3D can compute the main physical quantities of interest, namely, electromagnetic field distribution and the scattering cross-section, absorption cross-section and the total (extinction) cross-section. Importantly, since the frequency enters into the computations only through the electromagnetic constants of the particles (scatteres) OPTIMET-3D can practically be used for any frequency in the electromagnetic spectrum.

The second major feature of OPTIMET-3D is that it can describe the interaction of electromagnetic waves with periodic distribution of particles. This feature makes it particularly useful in studies of optical properties of photonic and plasmonic crystals and, more generally, for modelling photonic meta-materials. In particular, the software tool can be used to compute the transmission and reflection coefficients of a slab of photonic material and, consequently, the optical absorption in the slab, as well as the photonic band structure of the photonic material. As in the previous case, the particles in the unit

cell can have arbitrary shape and size and can be made of various optical materials, including metals, semiconductors and dielectrics.

The third major capability of OPTIMET-3D is that it can describe the non-linear interaction between electromagnetic waves and arbitrary distributions of particles made of centro-symmetric optical materials, such as noble metals and silicon. In this non-linear optical interaction, the electromagnetic field at the fundamental frequency (ω) gives rise to a field at the second harmonic (2ω), the field generation being confined primarily at the surface of particles or interfaces. This is perhaps the most important optical effect in non-linear optics, with many applications in surface optical spectroscopy, surface chemistry and optical biosensing. As in the linear case, the code provides the main physical quantities that characterise the (non-linear) interaction between the electromagnetic field and arbitrary distributions of particles, that is, the electromagnetic field distribution and the scattering cross-section, absorption cross-section and the extinction cross-section. We mention here that originally we intended to implement the simpler case, namely, that of *cubic optical nonlinearity*.

In addition to a high-performance, versatile code, this project has another major outcome, namely, it would play an important role in enhancing current scientific collaborations with worldwide leading academic groups working in nano-photonics and help to start new ones as well. In fact, we have already identified potential collaborations with Prof Jeremy Baumberg and Dr Ventsislav Valev from the University of Cambridge, in which OPTIMET-3D will be used to interpret experimental data regarding optical properties of self-assembled clusters of metallic nano-particles (more details about the scientific use of OPTIMET-3D are given in Sec. 7).

- As part of our ongoing research collaboration with Dr Paul Warburton's Group at UCL and Prof Richard Osgood's Group at Columbia University we plan to use OPTIMET-3D to study the non-linear optical properties of plasmonic meta-materials and non-linear photonic crystals. In particular, the software tool will be instrumental in advancing our work on next-generation solar cells that incorporate plasmonic materials.
- We will use OPTIMET-3D in our ongoing collaboration with Prof Chee Wei Wong's group at Columbia University, on multi-colour Anderson wave localisation in disordered ensembles of dielectric nano-particles.
- QPTIMET-3D will be instrumental in our ongoing collaboration with Prof Shuang Zhang's group at the University of Birmingham and Prof Xiang Zhang's group at Berkeley University (USA), *a project supported by EPSRC/NSF (EP/J018473/1),* on optical properties of classical and quantum meta-materials.

4. The Multiple Scattering Matrix Method

In order to facilitate the understanding of the main capabilities of OPTIMET-3D, we briefly present in this section the numerical method on which the code is based. Thus, the main steps of the MSM method can be described as follows: First, the incident, scattered, and internal (inside the scatterers) fields are expanded in Fourier series. The basis functions in 2D and 3D are multipole functions and VSWF, respectively [2-5]. Then, one constructs a system of linear equations whose unknowns are the Fourier coefficients of the scattered field. These coefficients are the main unknowns of the scattering problem as they can be used to compute most of the main physical quantities characterising the wave interaction, namely, the electromagnetic field distribution both inside and outside the scatterers, and the scattering, absorption and the extinction cross-sections.

This brief description of the MSM method shows that the main part of this algorithm consists in constructing and solving a system of linear equations whose unknowns are the Fourier coefficients of the scattered field. The matrix defining this system, also called the *transfer matrix* (or *T*-matrix), is completely defined by the location, shape and material parameters of the particles. The *T*-matrix of the system has a block structure, the corresponding blocks consisting of single-particle *T*-matrices and matrices that describe inter-particle interactions (coupling between particles). As a consequence of this block structure of the *T*-matrix, the MSM method can be easily applied to clusters with different number and distribution of particles. Equally important, the obvious scalability with the number of particles renders the MSM algorithm particularly suitable for parallelisation.

4.1 Mathematical Formulation of the Multiple Scattering Matrix Method

Consider a cluster of N particles being illuminated by a monochromatic plane electromagnetic wave. The origin of the co-ordinate system of the cluster is O and to each particle (j) one associates a co-ordinate system with the origin, O_j. The only constraint imposed on the location of the particles is that

the circumscribing spheres of the particles do not overlap, *i.e.* $|\boldsymbol{R}_{jl}| = |O_j - O_l| \geq \rho_j + \rho_l,\ j,l = 1,2,\dots,N, j \neq l$, where as per Fig. 1 ρ_j is the radius of the smallest sphere containing the *j*th particle.

The solution of the source-free Maxwell equations in 3D can be expanded in a complete basis of VSWFs, $\left(\boldsymbol{M}_{mn}^{(1)}, \boldsymbol{N}_{mn}^{(1)}\right)$ and $\left(\boldsymbol{M}_{mn}^{(3)}, \boldsymbol{N}_{mn}^{(3)}\right)$. In a practical implementation, the series is truncated to a certain order, n_{max}. Let $\sum_{mn} \stackrel{\text{def}}{=} \sum_{n=1}^{n_{max}} \sum_{m=-n}^{n}$; then, the incident, scattered and internal electric fields can be expressed as [2-5]:

incident field

$$\boldsymbol{E}_0^{inc}(\boldsymbol{R}) = \sum_{mn} \left[a_{mn} \boldsymbol{M}_{mn}^{(1)}(k\boldsymbol{R}) + b_{mn} \boldsymbol{N}_{mn}^{(1)}(k\boldsymbol{R}) \right], \tag{1}$$

internal field

$$\boldsymbol{E}^{int}(\boldsymbol{R}_j) = \sum_{mn} \left[c_{mn}^j \mathbf{Rg}\boldsymbol{M}_{mn}^{(1)}(k_j \boldsymbol{R}_j) + d_{mn}^j \mathbf{Rg}\boldsymbol{N}_{mn}^{(1)}(k_j \boldsymbol{R}_j) \right], \quad R_j < \rho_j,\ j = 1,2,\dots,N, \tag{2}$$

scattered field

$$\boldsymbol{E}^{sca}(\boldsymbol{R}_j) = \sum_{mn} \left[p_{mn}^j \boldsymbol{M}_{mn}^{(3)}(k\boldsymbol{R}_j) + q_{mn}^j \boldsymbol{N}_{mn}^{(3)}(k\boldsymbol{R}_j) \right], \quad R_j > \rho_j,\ j = 1,2,\dots,N, \tag{3}$$

where k and k_j are the wave vectors in the embedding medium and inside the *j*th particle, respectively, $\boldsymbol{R}$ and $\boldsymbol{R}_j, j = 1,2,\dots,N$, are the position vectors of a point, *P*, in the co-ordinate systems O and O_j, respectively. The magnetic field is subsequently obtained from the electric field as $\boldsymbol{H} = \boldsymbol{\nabla} \times \boldsymbol{E}$. The unknown expansion coefficients of the internal and scattered fields, $\left(c_{mn}^j, d_{mn}^j\right)$ and $\left(p_{mn}^j, q_{mn}^j\right)$, respectively, can be expressed in terms of the *known* expansion coefficients of the incident monochromatic plane wave, $\left(a_{mn}^j, b_{mn}^j\right)$, by imposing at the surface of the particles the boundary conditions satisfied by the electric and magnetic fields.

In the non-linear case, the corresponding electric field at the fundamental frequency (FF), $\boldsymbol{E}(\omega)$, gives rise to an electromagnetic field at the second harmonic (SH) frequency, $\Omega = 2\omega$. This field is generated by the non-linear dipoles described by the non-linear polarisation, $\boldsymbol{P}_\Omega$ [5,7,8]:

$$\boldsymbol{P}_\Omega = \boldsymbol{P}_\Omega^{surf} + \boldsymbol{P}_\Omega^{bulk}, \tag{4}$$

surface polarization

$$\boldsymbol{P}_\Omega^{surf} = \epsilon_0 : \chi_s^\Omega \boldsymbol{E}(\omega)\boldsymbol{E}(\omega)\delta\left(R - \rho_j\right), \tag{5a}$$

bulk polarization

$$\boldsymbol{P}_\Omega^{bulk} = \epsilon_0 \beta \boldsymbol{E}(\omega)\nabla \cdot \boldsymbol{E}(\omega) + \epsilon_0 \gamma \nabla[\boldsymbol{E}(\omega) \cdot \boldsymbol{E}(\omega)] + \epsilon_0 \delta[\boldsymbol{E}(\omega) \cdot \nabla]\boldsymbol{E}(\omega). \tag{5b}$$

For a rigorous derivation of Eqs. (5) the reader is referred to [8].

4.1.1 Single Particle Analysis

Let $\mathbf{a}^j = \left[a_1^j, a_2^j, \dots, a_{u_{max}}^j\right]^{\mathrm{T}}$, with $u_{max} = n_{max}^2 + 2n_{max}$, be a column vector, and define similarly $\mathbf{b}^j$, $\mathbf{c}^j$, $\mathbf{d}^j$, $\mathbf{p}^j$ and $\mathbf{q}^j$. Here, $\left(\mathbf{a}^j, \mathbf{b}^j\right)$, $\left(\mathbf{c}^j, \mathbf{d}^j\right)$ and $\left(\mathbf{p}^j, \mathbf{q}^j\right)$ represent the Fourier expansion coefficients of the incident, internal and scattered fields, respectively, defined with respect to O, relative to O_j, $j = 1,2,\dots,N$. Moreover, if one assumes that the system contains only the jth particle, a compact matrix representation of the Fourier coefficients of the electromagnetic fields, both inside and outside the particle, can be cast as follows [2]:

$$\begin{bmatrix} \mathbf{p}^j \\ \mathbf{q}^j \end{bmatrix} = \mathbf{T}^j \begin{bmatrix} \mathbf{a}^j \\ \mathbf{b}^j \end{bmatrix} = \begin{bmatrix} \mathbf{T}^{11} & \mathbf{0} \\ \mathbf{0} & \mathbf{T}^{22} \end{bmatrix}^j \begin{bmatrix} \mathbf{a}^j \\ \mathbf{b}^j \end{bmatrix}, \qquad \begin{bmatrix} \mathbf{c}^j \\ \mathbf{d}^j \end{bmatrix} = \mathbf{Q}^j \begin{bmatrix} \mathbf{a}^j \\ \mathbf{b}^j \end{bmatrix} = \begin{bmatrix} \mathbf{Q}^{11} & \mathbf{0} \\ \mathbf{0} & \mathbf{Q}^{22} \end{bmatrix}^j \begin{bmatrix} \mathbf{a}^j \\ \mathbf{b}^j \end{bmatrix}. \tag{6}$$

Here, $\mathbf{T}^j$ and $\mathbf{Q}^j$, $j = 1,2,\dots,N$, are the *scatterer-centred T*-matrix of the *j*th particle and a matrix that relates the Fourier coefficients of the inside and outside fields, respectively. Note that the block-diagonal structure of the $\mathbf{T}^j$ and $\mathbf{Q}^j$ matrices is valid only for spherical particles.

4.1.2 Multiple Particles System

The central idea of the Foldy–Lax multiple scattering theory [9] is that in the vicinity of any scatterer *j* in the *N* particle system, there is a local field that is the superposition of the incident field and the field scattered by all the other scatterers in the system, except the scatterer itself. Using the definition of the single-particle *T*-matrix, $\mathbf{T}^j$, $j = 1,2,\dots,N$, the Fourier expansion coefficients of the scattered and incident fields, $\left(\mathbf{p}^j, \mathbf{q}^j\right)$ and $\left(\mathbf{a}^j, \mathbf{b}^j\right)$, respectively, obey the following equation:

$$\begin{bmatrix}\mathbf{p}^j\\ \mathbf{q}^j\end{bmatrix} = \mathbf{T}^j\left\{\begin{bmatrix}\mathbf{a}^j\\ \mathbf{b}^j\end{bmatrix} + \sum_{l\neq j}\begin{bmatrix}\mathbf{p}^{lj}\\ \mathbf{q}^{lj}\end{bmatrix}\right\}, \qquad j = 1,2,\dots,N. \tag{7}$$

The coefficients $(\mathbf{a}^j, \mathbf{b}^j)$ and $(\mathbf{p}^{lj}, \mathbf{q}^{lj})$, where $\mathbf{p}^{lj} = \left[p_1^{jl}, p_2^{lj}, \dots, p_{u_{max}}^{lj}\right]^{\mathrm{T}}$, and similarly for $\mathbf{q}^{lj}$, need to be expressed in terms of the known expansion coefficients of the incoming field and $(\mathbf{p}^j, \mathbf{q}^j)$, respectively, which are calculated in the system with the origin in O. This is achieved by using the vector translation-addition theorem [2, 4]. Thus, let us consider the matrix coefficients,

$$\alpha^{(j,l)} = \begin{bmatrix}A^{(3)}\left(k\boldsymbol{R}_{jl}\right) & B^{(3)}\left(k\boldsymbol{R}_{jl}\right)\\ B^{(3)}\left(k\boldsymbol{R}_{jl}\right) & A^{(3)}\left(k\boldsymbol{R}_{jl}\right)\end{bmatrix}, \qquad j,l = 1,2,\dots,N,\ \ j\neq l, \tag{8a}$$

$$\beta^{(j,0)} = \begin{bmatrix}A^{(1)}\left(k\boldsymbol{R}_{j0}\right) & B^{(1)}\left(k\boldsymbol{R}_{j0}\right)\\ B^{(1)}\left(k\boldsymbol{R}_{j0}\right) & A^{(1)}\left(k\boldsymbol{R}_{j0}\right)\end{bmatrix}, \qquad j = 1,2,\dots,N, \tag{8b}$$

where $A^{(z)}(k\boldsymbol{R})$ and $B^{(z)}(k\boldsymbol{R})$, $z = 1,3$, represent the vector translation-addition coefficients, which are evaluated using an efficient recursive implementation as proposed in [4]. Let $\mathbf{f}^j = \left[\mathbf{p}^j\ \mathbf{q}^j\right]^{\mathrm{T}}$ and $\mathbf{A} = [\mathbf{a}\ \mathbf{b}]^{\mathrm{T}}$. Then, the single-particle scattering expansion coefficients, $\mathbf{f}^j$, can now be expressed in terms of $\mathbf{A}$ and $\mathbf{f}^l$, $j,l = 1,2,\dots,N, j\neq l$, as:

$$\mathbf{f}^j = \mathbf{T}^j\beta^{(j,0)}\,\mathbf{A} + \mathbf{T}^j\sum_{l\neq j}\alpha^{(j,l)}\mathbf{f}^l. \tag{9}$$

In terms of the known Fourier expansion coefficients of the incident field, $\mathbf{A}$, the resulting system of linear equations for the N particle system for the unknown Fourier expansion coefficients of the scattered field, $\mathbf{f}^j$, $j = 1,2,\dots,N$, can be expressed in the following form:

$$\begin{bmatrix}\mathbf{I} & -\mathbf{T}^1\alpha^{(1,2)} & -\mathbf{T}^1\alpha^{(1,3)} & -\mathbf{T}^1\alpha^{(1,4)} & \dots & -\mathbf{T}^1\alpha^{(1,N)}\\ -\mathbf{T}^2\alpha^{(2,1)} & \mathbf{I} & -\mathbf{T}^2\alpha^{(2,3)} & -\mathbf{T}^2\alpha^{(2,4)} & \dots & -\mathbf{T}^2\alpha^{(2,N)}\\ -\mathbf{T}^3\alpha^{(3,1)} & -\mathbf{T}^3\alpha^{(3,2)} & \mathbf{I} & -\mathbf{T}^3\alpha^{(3,4)} & \dots & -\mathbf{T}^3\alpha^{(3,N)}\\ -\mathbf{T}^4\alpha^{(4,1)} & -\mathbf{T}^4\alpha^{(4,2)} & -\mathbf{T}^4\alpha^{(4,3)} & \mathbf{I} & \dots & -\mathbf{T}^4\alpha^{(4,N)}\\ \vdots & \vdots & \vdots & \vdots & \ddots & \vdots\\ -\mathbf{T}^N\alpha^{(N,1)} & -\mathbf{T}^N\alpha^{(N,2)} & -\mathbf{T}^N\alpha^{(N,3)} & -\mathbf{T}^N\alpha^{(N,4)} & \dots & \mathbf{I}\end{bmatrix}\begin{bmatrix}\mathbf{f}^1\\ \mathbf{f}^2\\ \mathbf{f}^3\\ \mathbf{f}^4\\ \vdots\\ \mathbf{f}^N\end{bmatrix} = \begin{bmatrix}\mathbf{T}^1\beta^{(1,0)}\mathbf{A}\\ \mathbf{T}^2\beta^{(2,0)}\mathbf{A}\\ \mathbf{T}^3\beta^{(3,0)}\mathbf{A}\\ \mathbf{T}^4\beta^{(4,0)}\mathbf{A}\\ \vdots\\ \mathbf{T}^N\beta^{(N,0)}\mathbf{A}\end{bmatrix}. \tag{10}$$

The system (10) can be expressed in a compact matrix form, $\mathbf{S}_\omega\mathbf{F}_\omega = \mathbf{U}_\omega$, where $\mathbf{F}_\omega = [\mathbf{f}^1, \mathbf{f}^2, \dots, \mathbf{f}^N]^{\mathrm{T}}$, $\mathbf{U}_\omega = \left[\mathbf{T}^1\beta^{(1,0)}\mathbf{A}, \mathbf{T}^2\beta^{(2,0)}\mathbf{A}, \dots, \mathbf{T}^N\beta^{(N,0)}\mathbf{A}\right]^{\mathrm{T}}$ and $\mathbf{S}_\omega$ denotes the FF (linear) scattering matrix of the system. ***Constructing the system matrix $\mathbf{S}_\omega$ and solving Eq. (10) represent the core parts of the MSM method***. Similarly, in the non-linear case the scattering problem is reduced to solving a system of linear equations, $\mathbf{S}_\Omega\mathbf{F}_\Omega = \mathbf{U}_\Omega$, where $\mathbf{S}_\Omega$ and $\mathbf{F}_\Omega$ are the (non-linear) scattering matrix of the system and the Fourier expansion coefficients of the (non-linear) scattered field, respectively.

4.1.3 Periodic Arrays of Particles

Consider an infinitely extended, 2D periodic lattice of particles situated in the *xy*-plane, defined by the Bravais lattice vectors $\boldsymbol{R}_n = n_1\boldsymbol{a}_1 + n_2\boldsymbol{a}_2$, where $n_1, n_2 = 0, \pm1 \pm 2, \dots$ and $(\boldsymbol{a}_1, \boldsymbol{a}_2)$ are the basis vectors of the lattice. The corresponding reciprocal lattice is defined by $\boldsymbol{g}_m = m_1\boldsymbol{b}_1 + m_2\boldsymbol{b}_2$, where $m_1, m_2 = 0, \pm1 \pm 2, \dots$ and $(\boldsymbol{b}_1, \boldsymbol{b}_2)$ are the basis vectors of the reciprocal lattice. $(\boldsymbol{a}_1, \boldsymbol{a}_2)$ and $(\boldsymbol{b}_1, \boldsymbol{b}_2)$ are related through the relations $\boldsymbol{a}_i \cdot \boldsymbol{b}_j = 2\pi\delta_{ij}, i,j = 1,2$.

The solution for the scattered electromagnetic field for an arbitrary 2D lattice can be efficiently obtained *via* the lattice-centre translation-addition theorem, which replaces the contribution of each particle with an equivalent contribution of a particle located at $\boldsymbol{R}_0 = 0$ [10,11]. Then, the total scattered field, $\boldsymbol{E}_{\boldsymbol{g}}^{sc}$, is obtained from the reciprocal lattice identity relationship, which expresses the VSWFs expansion in the $\boldsymbol{R}_n$ lattice in the limit $n \to \infty$ in an equivalent form as a truncated expansion in the reciprocal lattice [10,11]:

scattered field

$$\boldsymbol{E}_{\boldsymbol{g},i}^{sca,s} = \sum_{\boldsymbol{g}',i',s'}\mathbf{M}_{\boldsymbol{g}i,\boldsymbol{g}'i'}^{s,s'}\,\boldsymbol{E}_{\boldsymbol{g}',i'}^{inc,s'}, \tag{11}$$

where i and i' denote Cartesian components, $s, s' = \pm 1$ denote the direction of the incident field, $\boldsymbol{E}^{inc}$, for $z > 0$ $(s = 1)$ and $z < 0$ $(s = -1)$. The analytical expressions for $\mathbf{M}^{s,s'}_{\boldsymbol{g}i,\boldsymbol{g}'i'}$ are given in [10,11]. From these expressions the transmitted and reflected fields from the 2D lattice are:

transmitted field

$$\boldsymbol{E}^{trans}_{\boldsymbol{g},i} = \sum_{\boldsymbol{g}',i'} \mathbf{M}^{+,+}_{\boldsymbol{g}i,\boldsymbol{g}'i'}\, \boldsymbol{E}^{inc,+}_{\boldsymbol{g}',i'}, \tag{12}$$

reflected field

$$\boldsymbol{E}^{refl}_{\boldsymbol{g},i} = \sum_{\boldsymbol{g}',i'} \mathbf{M}^{-,+}_{\boldsymbol{g}i,\boldsymbol{g}'i'}\, \boldsymbol{E}^{inc,+}_{\boldsymbol{g}',i'}, \tag{13}$$

where the corresponding transmittance and reflectivity of the 2D lattice (slab) are defined as the ratio of the fluxes of $\boldsymbol{E}^{trans}_{\boldsymbol{g}}$ and $\boldsymbol{E}^{refl}_{\boldsymbol{g}}$, respectively, to the flux of $\boldsymbol{E}^{inc}$ (note that the sum over the diffraction orders i has been taken out). The details of the implemented code, OPTIMET-3D, and the associated parallelisation strategy are presented in the next section.

5. Technical Implementation of OPTIMET-3D

In this section, the technical implementation of OPTIMET-3D and several parallelisation strategies employed for its numerical acceleration are presented. Then, the structural framework of the software is given with a comprehensive description of the major building blocks of the code.

5.1 Technical Overview

OPTIMET-3D is written in C++ programming language. We have employed the standard Object Oriented Programming (OOP) framework, namely, *the one class, one source file, one header strategy* is followed (see also Fig. 2), in order to allow increased flexibility in the code writing, code extension and its future development, as well as to facilitate a distributed revision control.

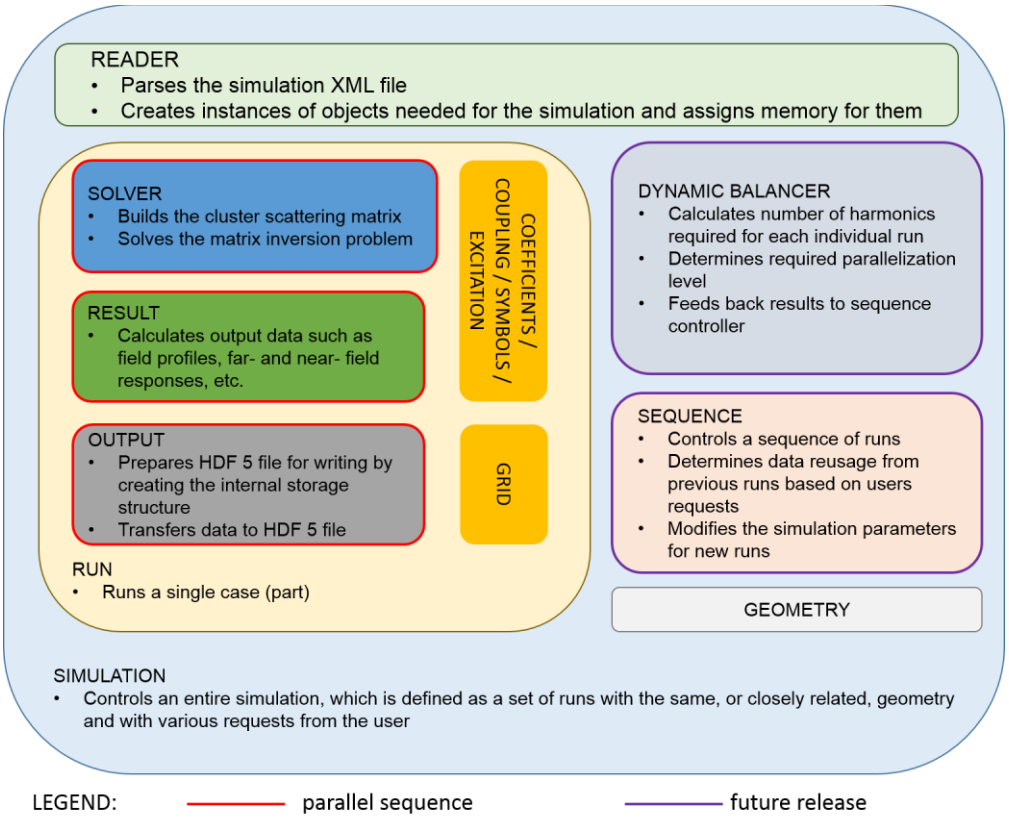

***Figure 2**. Structural block-diagram of OPTIMET-3D. Each block in the framework of the code corresponds to a single C++ class.*

In the code development work, we used DOXYGEN documentation system, which integrates very well within the OOP framework. It dynamically generates an interactive documentation of the resulting API. The associated documentation is available in both HTML and PDF formats.

For the end users, those who do not intend to develop their own simulations using the API, OPTIMET-3D has a very simple and flexible input system based on a single XML file. For this, we use *pugixml*, a lightweight and fast, open source XML parser that can be found at https://code.google.com/p/pugixml/. The user is required to define XML blocks such as simulation parameters, geometry and incoming wave. Each of these blocks contains sub-blocks, which can hold, for example, object definitions such as position, electromagnetic properties, particle size, etc. A short guide explaining how to write an input file is made available with the code. It should be noted that due to the popularity of XML as a data description solution, many graphical interfaces exist for building XML files. Therefore, it would be trivial to create a user-friendly GUI for all data input.

In terms of deployment, we use the CMake system in order to enhance the portability of OPTIMET-3D and facilitate its installation on a given HPC system. CMake is an automated *makefile* generator, which searches for existing libraries on the target system and builds an appropriate *makefile* to compile the software. Currently, OPTIMET-3D requires four major components for it to work: an MPI library, a mathematical library that offers LAPACK and BLAS (ScaLAPACK, PBLAS and BLACS for the parallel version), the GNU Scientific Library and the HDF5 library. CMake uses *finders*, which are simple script files, to locate static and dynamic objects, as well as header files. Currently, the *finders* support OpenMPI, Intel's MPI and MPICH for the parallel communication libraries, and Intel's MKL, IBM's ESSL and the Armadillo Linear Algebra Pack for accessing the mathematical subroutines. Finally, it should be noted that both GSL and HDF5 are open-source packages, which are available on most scientific computing systems.

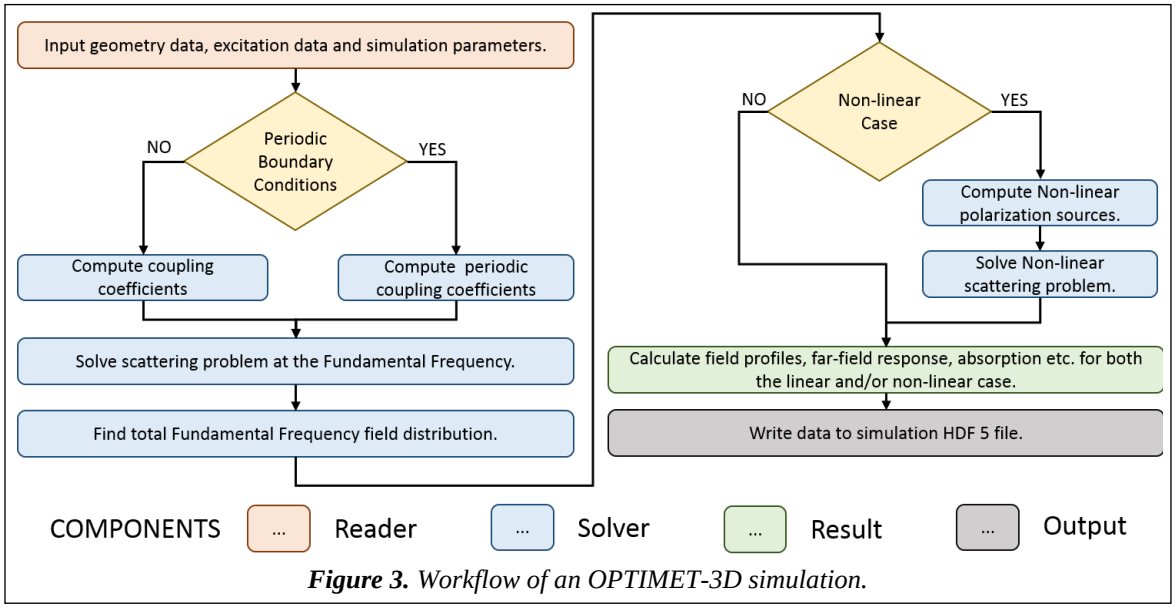

Figure 3. *Workflow of an OPTIMET-3D simulation.*

In order not to burden the user with editing *makefiles* or to be concerned over the resulting linkage order and linking targets, the CMake system provides ideal functionality for improved code portability. The associated CMake scripts have been tested on several HPC platforms, so far, including UCL's *Legion* and the InfraGrid and BlueGene/P HPC systems at the West University of Timisoara. Moreover, it is rather straightforward to manually add additional support for a new system or library. For example, in order to add support for the AMD's mathematical libraries, the user simply has to change the linear algebra finder script in order to point to these new libraries. In addition, in the use of CMake, the user has the option to specify a number of flags in order to indicate support for the statically or dynamically linked libraries and to choose the parallel or serial branch of the code.

Finally, we use the Mercurial revision control system in order to facilitate access to all revisions of the code, as well as the up to date API documentation.

5.2 Structural Framework

As we have explained, OPTIMET-3D strictly follows OOP framework guidelines. Specifically, each single component of the code is defined as a separate class with its own header file. Classes that have to perform data storage operations are given two main access methods, an `init()` method, which allocates any necessary memory for the data storage and initialises the object, and a `populate()` method, which populates the data storage attributes of the object based on the initialisation parameters and the role of the object. Classes that have no data storage role are declared with all members `static`

in order to allow easy access to them and eliminate any confusion as to the need of instantiation. A schematic overview of the structural framework of OPTIMET-3D is presented in Fig. 2, whereas the workflow associated with a typical OPTIMET-3D simulation and the corresponding features of the code are shown in Fig. 3.

The main classes defined in the framework of OPTIMET-3D are:

- `Algebra` – defines wrappers to linear algebra and vector-vector and vector-matrix operations solvers based on the available mathematical libraries (currently supports BLAS, LAPACK, GSL, MKL, ESSL, Armadillo); ***includes parallel version.***
- `Coefficients` – computes all expansion coefficients needed for vector spherical components, including the ***M*** and ***N*** vector functions, and the Wigner *d*-functions.
- `Coupling` – computes electromagnetic coupling coefficients between particles, specifically, $\alpha^{(j,l)}$ and $\beta^{(j,l)}$ transfer matrix coefficients, which are used to transform vector spherical functions between co-ordinate systems.
- `PeriodicCoupling` – this class is identical to the `Coupling` class in terms of usage and scope, but it is used as a replacement for the former when periodic boundary conditions are employed in simulations.
- `Excitation` – defines an incoming electromagnetic excitation, including expansion coefficients and polarisation state (currently supports plane wave excitations with Gaussian pulsed excitation [12] being planned for a future release).
- `Geometry` – stores all data defining the cluster geometry (including electromagnetic properties). It also stores for each scatterer the Fourier expansion coefficients of the internal electromagnetic fields.
- `Output` – provides a versatile interface to set up the internal structure of the HDF5 output file of the simulation, as well as input/output data transfer to this file; ***includes parallel version.***
- `OutputGrid` – defines spatial grids for 3D field output and visualisation. The current version supports regular and iregular cartesian grids. Spherical and cylindrical co-ordinate grids will be provided in a future release.
- `Reader` – parses the simulation XML file and sets up all of the needed objects, including the `Geometry`, `Excitation`, `Output` and `OutputGrid` objects (the latter one is used only in cases where field results are requested).
- `Result` – calculates required physical data from the Fourier expansion coefficients (*i.e.* scattering and internal expansion coefficients) provided by the `Solver`. Currently the software calculates field profiles, near- and far-field cross-sections, and performs wavelength scans; ***includes parallel version.***
- `Run` – provides an interface to run a single instance of the solver (*i.e.* using a fixed geometry and excitation source).
- `Simulation` – overall control and monitoring class. Ideally, this should be the only class with which a user of the API needs to interact directly, as once instantiated it provides access to the `Geometry`, `Excitation`, `Solver`, `Result` and `Output` classes.
- `Solver` – solves system of linear equations corresponding to the linear or non-linear scattering problem and feeds the solution to a `Result` object; ***includes parallel version.***
- `Symbol` - provides static members to compute several symbols and special functions required by the numerical formalism (*e.g.*, 3*j*, 6*j* and 9*j* Wigner symbols, Clebsch-Gordan coefficients and the C-symbols required for computing the non-linear sources).
- `Sequence` – provides an interface that allows the user to create a series of *requests* from the simulation point of view (*e.g.*, specific field profiles, cross-sections, wavelength scans, etc.). The role of this class is to ensure that no extra work is being spent on computing any data that may not be needed (*e.g.*, there is no point in calculating the internal field coefficients when only the linear far-field response is requested).
- `Balancer` – provides a dynamic balancer that, for each scatterer, automatically calculates the maximum number of harmonics required for convergence (based on the electromagnetic and geometrical properties of the particular scatterer). This in turn determines the level of parallelisation required, based on the number of scatterers and nodes available, as well as the resources allocated to each node. The outcome is then fed back to the `Sequence` controller; ***this class is planned for a future release as it requires comprehensive testing.***

5.3 Parallel Implementation

The basic characteristics of the multiple scattering matrix method renders the algorithm implemented as OPTIMET-3D highly parallelisable, scalable and stable. The software setup does not suffer from race conditions and encapsulates highly uniform data structures, which potentially allow for straightforward achievement of load balancing.

The primary challenge that arises when performing complex numerical simulations, namely, those which involve the study of a large number of scatterers, is the need for a large amount of memory required for storing the system scattering matrix, *i.e.* $\mathbf{S}_{\omega}$ or $\mathbf{S}_{\Omega}$. In order to illustrate these memory requirements, the size of the scattering matrix approaches 6 GB for a cluster of 13 particles with $n_{max} = 20$ harmonics. In our calibration, this is considered a large memory requirement, in particular, when considering a parallel clusters where, typically, the *per node* memory size ranges between 2 GB and 4 GB. In addition, as the distance between any two scatterers in the cluster increases, in order to obtain accurate convergence in the VSWF translation calculations, n_{max} must be increased as well. To be more specific, in some cases up to 40 harmonics or more may be required. Furthermore, as several of our envisioned science related applications of OPTIMET-3D will require randomly distributed ensembles of hundreds of particles, employing a distributed computing method relying on splitting the memory cost of storing the scattering matrix among available nodes becomes mandatory.

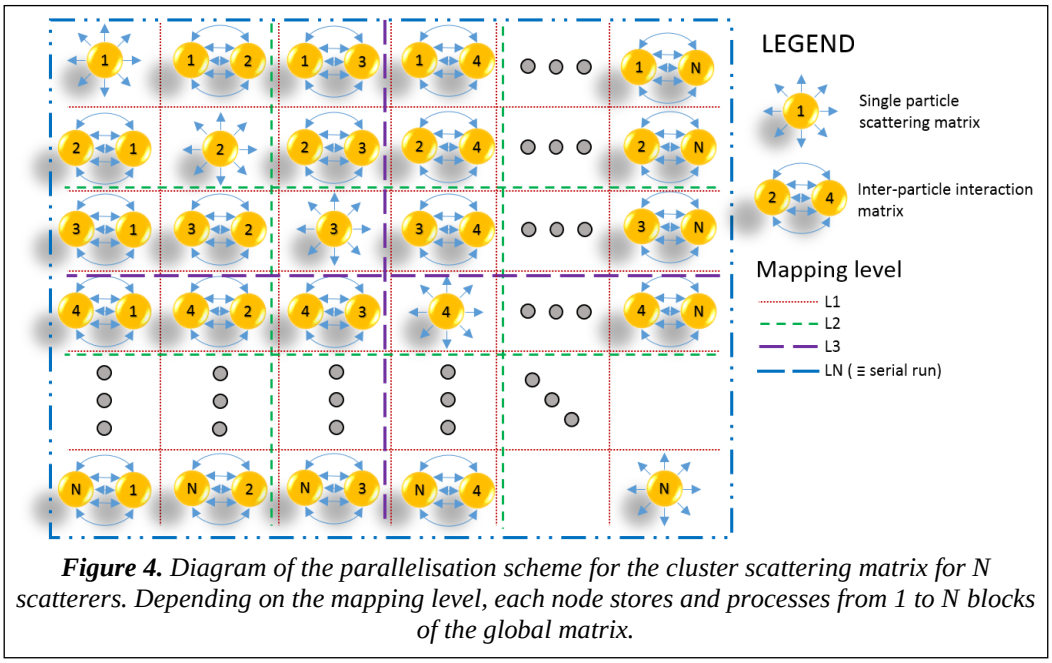

Figure 4. *Diagram of the parallelisation scheme for the cluster scattering matrix for N scatterers. Depending on the mapping level, each node stores and processes from 1 to N blocks of the global matrix.*

The algorithm used to distribute the memory is schematically depicted in Fig. 4. The most basic and most natural memory split is *per bi-particle interaction level*. Each node holds the part of the matrix that describes either the single scattering matrix, $\mathbf{T}^j$, or the inter-particle interaction matrix. We denote this scheme as ***Level 1*** (L1) parallelisation strategy. While L1 is straightforward to implement and uses efficiently the intrinsic symmetries in the scattering matrix formalism, it has several drawbacks. First, whilst the cluster scattering matrix is large, the distributed components only take a few hundreds of MB in memory storage, thus, each node only uses a fraction of its available resources. Second, the number of required nodes scales quadratically with the number of scatterers in the system. As a result, for the relatively simple case of a cluster with 20 particles, 400 nodes are required to implement an L1 parallelisation strategy. For HPC systems of the size of *Legion* this might not be practical (on *Legion* the cores requirement of a typical job cannot exceed ~200).

In addition to the L1 parallelisation scheme, where each basic block is distributed to a node, higher levels of matrix distribution have been considered, as illustrated in Fig. 4. Each level L*m* distributes an $m \times m$ block matrix to each node. In this notation, for a given cluster with N particles, when $m = N$ the algorithm implementation simply becomes a serial one. Thus, by allowing a flexible use of higher-order parallelisation levels, OPTIMET-3D software can use efficiently the available resources whilst allowing complex simulations to run on smaller number of nodes. We refer to this type of parallel mapping as *balanced mapping*.

One issue that arises with a higher level of parallelisation is the unbalanced distribution of the scattering matrix when it is not exactly mapped to the available nodes by square-block matrices (*i.e.* when the

number of scatterers N is not an integer multiple of the parallelisation level m). This situation is illustrated in Fig. 5. To simplify the presentation of this case, consider a very basic cluster of 5 scatterers, whose scattering matrix contains $5 \times 5 = 25$ elemental blocks. The first 16 elemental blocks of the 25 block matrix are distributed according to an L2 mapping, whereas the remaining 9 blocks are mapped as a column and row block matrices. Note that the last node will have an additional block to process. This is usually of a limited concern since the corresponding block components are independent. Therefore, no race condition occurs. It has been observed during our numerical experiments that for $n_{max} = 40$, a 4×4 matrix requires less than 2 GB, thus making very useful the L4 and L3 mapping schemes. As a consequence, this *edge mapping scheme* can be used for particle

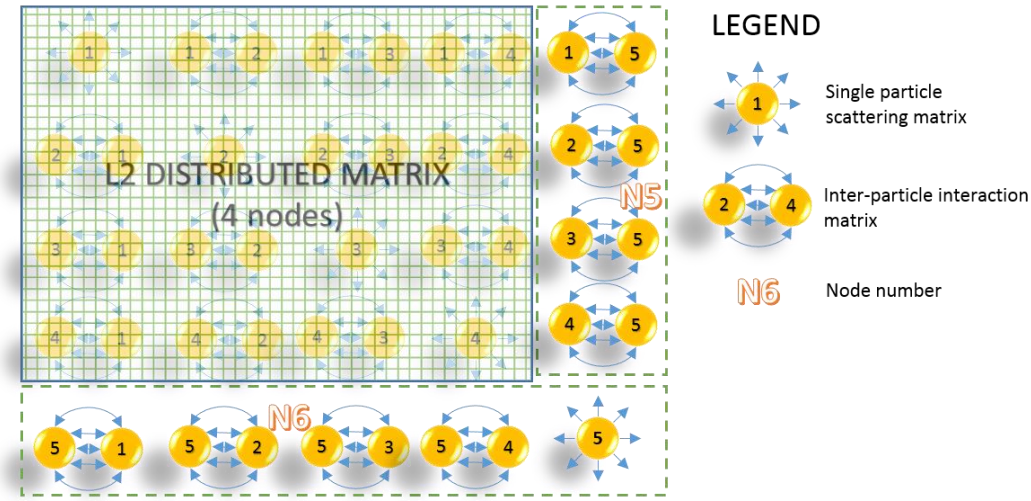

Figure 5. *Example of "edge" distribution of the scattering matrix elements in an unbalanced mapping case. The geometry consists of 5 particles. The first 4 blocks of the scattering matrix are mapped with the L2 scheme whilst the remaining blocks are distributed as shown.*

clusters that have the property $N = 3k + 1$, where k is an arbitrary integer. In addition, edge mapping can be used for any odd number of scatterers. Nevertheless, for $n_{max} = 40$, the resulting size of a block is less than 1 GB. This makes the Lm scheme practical for the relatively older generation of computing systems; however, it may lead to resource wasting on newer clusters. To this end, the following *hybrid mapping scheme* is proposed.

The hybrid mapping scheme combines several balanced mapped areas of different levels, as well as row and column mapping in order to cover the entire scattering matrix of the system, as per Fig. 6. The hybrid mapping scheme proves to be the most effective mapping model in terms of resource balancing.

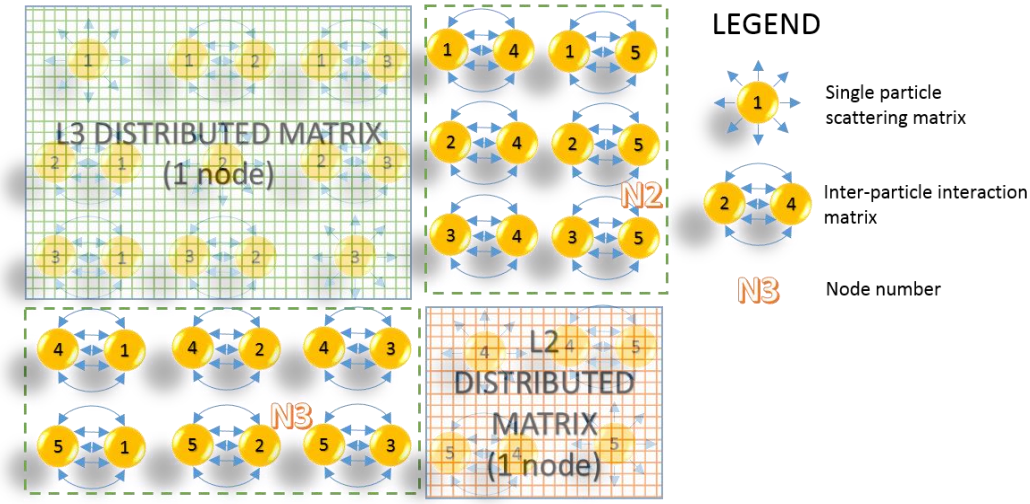

Figure 6. *Schematic of the hybrid mapping strategy. The example considered is for $N = 5$ particles. Note that this is one of several possible hybrid mapping strategies for this particular N.*

However, one does not expect the user to create the corresponding map, so that an automatic mapping scheme must be implemented. As a result, this is no longer as simple a matter as it is in the case of the edge and balanced mapping schemes, so that its implementation has been left for a future release.

At the time of writing this report, OPTIMET-3D software supports L1 and all the balanced mapping schemes. The edge mapping scheme is currently being investigated for implementation. As such, the hybrid mapping scheme will be made available at a later release of the software. It is also noted that the issue of matrix mapping is a well-known research topic in parallel computing, where several algorithms and engines are available for this purpose. In the future development of OPTIMET-3D, we intend to use such technologies as seen feasible.

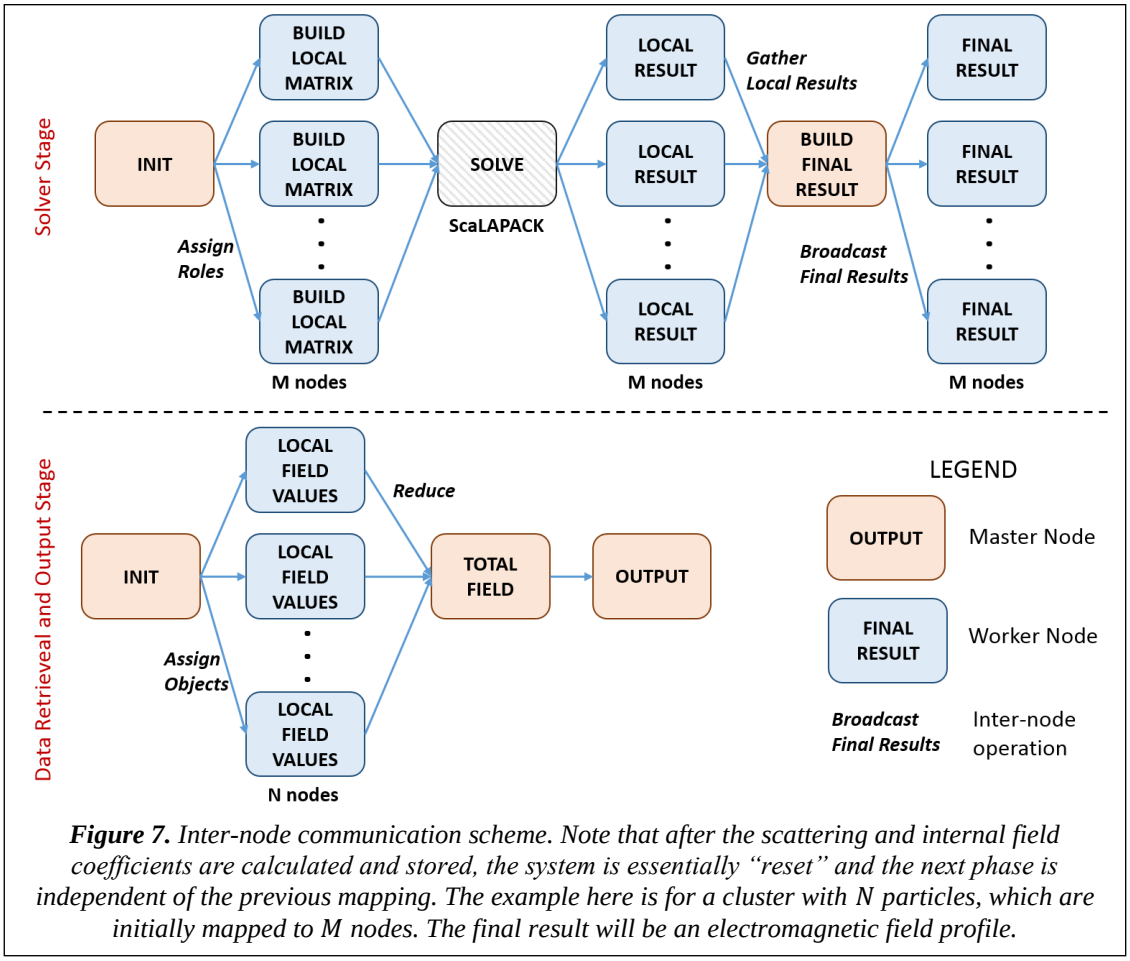

Figure 7. *Inter-node communication scheme. Note that after the scattering and internal field coefficients are calculated and stored, the system is essentially "reset" and the next phase is independent of the previous mapping. The example here is for a cluster with N particles, which are initially mapped to M nodes. The final result will be an electromagnetic field profile.*

The inter-node communication processes of OPTIMET-3D are illustrated in Fig. 7. In what follows, we give a brief description of these processes. After the *Master* node initialises the simulation and chooses the appropriate parallelisation strategy, the *Worker* nodes are each assigned a piece of the scattering matrix to be build, *i.e*, a part of $\mathbf{S}_\omega$ or $\mathbf{S}_\Omega$. Each *Worker* builds independently its assigned piece of the matrix. The first N nodes, N being the number of particles in the system, are then assigned the system matrix $\mathbf{S}_\omega$ or $\mathbf{S}_\Omega$, at which point ScaLAPACK is called to solve the scattering matrix equation. Finally, the *Master* node gathers the individual results from each of the N nodes and builds the solution vector containing the Fourier expansion coefficients of the scattered field. The *Master* node also calculates the internal field coefficients for each particle. This last step can also be computed in parallel; however, numerical tests have shown it to be of a reduced computational cost. Thus, in order to keep the inter-node communication to a minimum, this operation is performed on the *Master* node only. Finally, the *Master* node updates the `Geometry` object to include the newly computed internal coefficients, which then broadcasts both the internal coefficients and the solution vector to the remaining $M - N$ nodes.

At this point, the nodes are ready to perform all other calculations that the user has requested. For the field profile, for example, each node calculates the contribution from its own assigned object and then the *Master* performs a reduce operation in order to retrieve the total field on the grid. As the field point locations are independent, more than N nodes can be used for this computation, where the individual grid points for each node to compute are selected. In the case of a wavelength scan, for example, each node is assigned a portion of the spectrum for which it calculates the far- and/or near-field responses. Each node can then individually output the result to a single HDF5 file by using the parallel output system, which is implicitly implemented by HDF5. It is reiterated that no race condition occurs and that the load balancing is ensured by enforcing that each node is assigned to compute an equal work load from the desired spectrum of frequencies.

For the non-linear response calculations, a parallelisation strategy similar to the one employed in the linear case is used. However, in this case each node needs to communicate the corresponding non-linear source terms of their assigned particle(s) to all the other nodes. The *Master* process does not require any additional information to compute the non-linear response because once the non-linear scattering coefficients are known, the formalism is identical to that of the linear response calculations.

The parallelisation tasks in OPTIMET-3D are provided *via* MPI. The mathematical computations (*i.e.* linear algebra operations), which require parallelisation are implemented through ScaLAPACK. In this particular case, all associated inter-process communications are invoked by BLACS, which provides a very cost effective interface for transferring among the nodes all data required. In this implementation, ScaLAPACK and BLACS are chosen because they are provided as the standard implementation of parallel algebra computations in all major mathematical library distributions, including Intel's MKL and IBM's ESSL. In addition, both packages are freely available from the *netlib* repository.

Finally, it should be mentioned that we have also explored briefly the possibility of porting OPTIMET-3D onto GPU-based clusters, such as *nVidia*'s Fermi architecture. Preliminary investigations have shown that this code development would be very attractive, both due to the enhancement of the functionality of the software, and, equally important, because of the increase in the deployment base and potential of the software.

6. Performance and Scalability Analysis

As presented in the previous section, due to the high degree of parallelisability of the MSM algorithm OPTIMET-3D is expected to perform very well when ported onto a parallel computing environment. We have performed several performance tests for the level of mapping, Lm, $m = 1,2,3$, using a series of clusters of spherical particles. The number of particles in the cluster was N_p, $p = \{1, 2, \dots, 12\}$. The output data was the field profile on a 3×3 grid section located at the centre of the cluster but outside of any of the spheres. This was done in order to ensure that the actual performance data was related to the solver and not to any I/O processes. In addition, the strong scalability of the parallelised OPTIMET-3D solver was tested for the case of $N_p = 12$.

6.1 Performance Analysis

The focus of this section is the investigation of the parallelised branch of OPTIMET-3D when different mapping levels, Lm, and corresponding number of nodes, N_n are used. In Sec. 5.3, it was explained that different Lm schemes would lead to different resource usage conditions. In particular, it was concluded that the number of processing nodes required, N_n, decreases as Lm increases. Moreover, when one

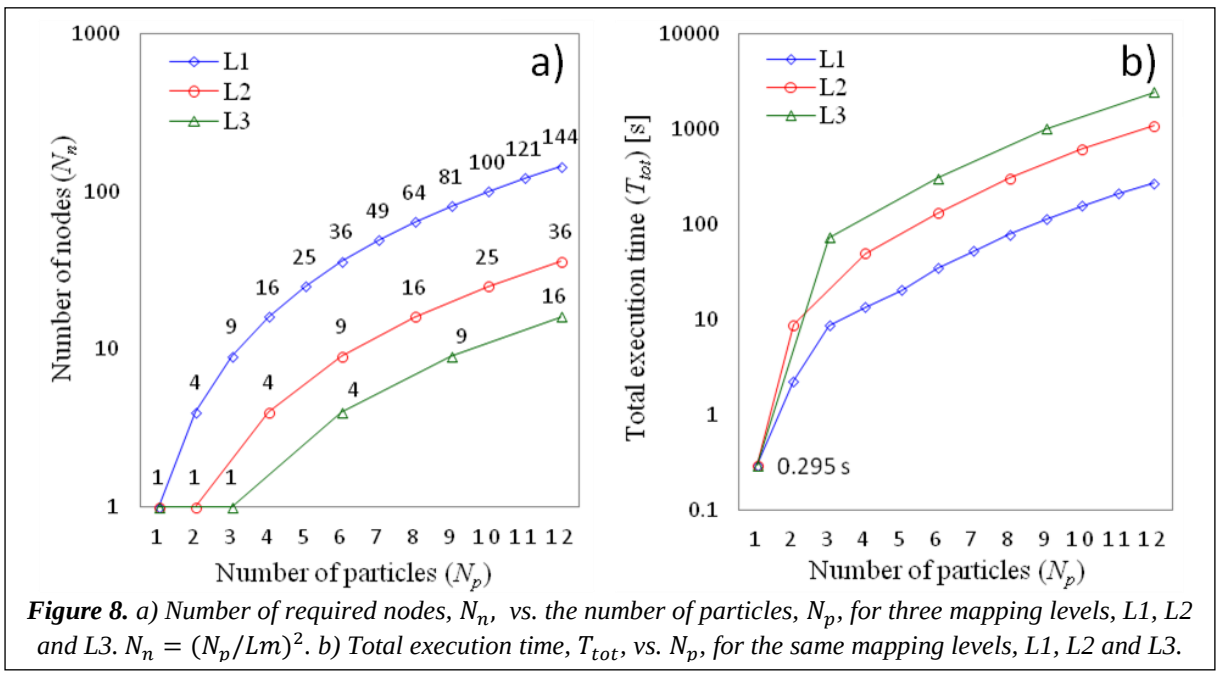

Figure 8. *a) Number of required nodes, N_n, vs. the number of particles, N_p, for three mapping levels, L1, L2 and L3. $N_n = (N_p/Lm)^2$. b) Total execution time, T_{tot}, vs. N_p, for the same mapping levels, L1, L2 and L3.*

considers modern HPC systems, where the associated memory available is typically below 4 GB per N_n, our tests have demonstrated that L3 is an optimal choice. However, L2 can also be used efficiently in conjunction with the edge mapping strategy, if all possible distribution scenarios can be accounted for. Finally, L1 mapping is the most efficient mapping strategy in terms of total execution time, T_{tot};

however, this is achieved at the expense of a larger number N_n of nodes being used. Thus, one has to bear in mind this trade-off when using L1, as overall it could be regarded as being the least cost effective of all schemes. In all simulations performed in this work, T_{tot} includes both the computation time and communication time.

In order to illustrate how the number of required computing nodes, N_n, scale with the number of particles in the cluster, N_p, we plot in Fig. 8(a) the dependence $N_n = (N_p/Lm)^2$ for three mapping orders, Lm, $m = 1,2,3$. The cluster size is characterised by the number of spheres, $N_p = 1, \ldots, 12$. For the case with $N_p = 12$ particles, it is observed that the L1 strategy requires $N_n = 144$ nodes, whilst N_n decreases to $N_n = 36$ and $N_n = 16$ for the L2 and L3 schemes, respectively.

In terms of the total execution time, T_{tot}, we have run the test cases detailed above, as per Fig. 8(b), on the *Legion* cluster at UCL. The number of harmonics used was $n_{max} = 30$, which provides a typical value for simulations of average complexity. We would expect that in most cases n_{max} ranges from $n_{max} = 5$ if dielectric particles are considered to $n_{max} = 40$ in the case of metallic particles. In the latter case a larger n_{max} is required both due to increased permittivity of metals and the excitation of strong optical resonances. As expected, L1 mapping level offers the lowest execution time, for example, for the cluster with $N_p = 12$ spheres, $T_{tot} = 271$s. L3, on the other hand, shows on average a 9 fold increase of the same simulation, namely, for $N_p = 12$, $T_{tot} = 2441$ s. This result is explained by the fact that for $N_p = 12$, L3 scheme employs only $N_n = 16$ nodes, as opposed to the L1 schemes, which requires $N_n = 144$ nodes. It can be seen that the decrease in the number of required nodes is exactly equal to 9. It should be noted that the small discrepancies are attributable to non-uniform execution times due to ScaLAPACK's speed improvements, which are found to slightly depend on the particular content of the scattering matrix and the associated inter-node communication costs.

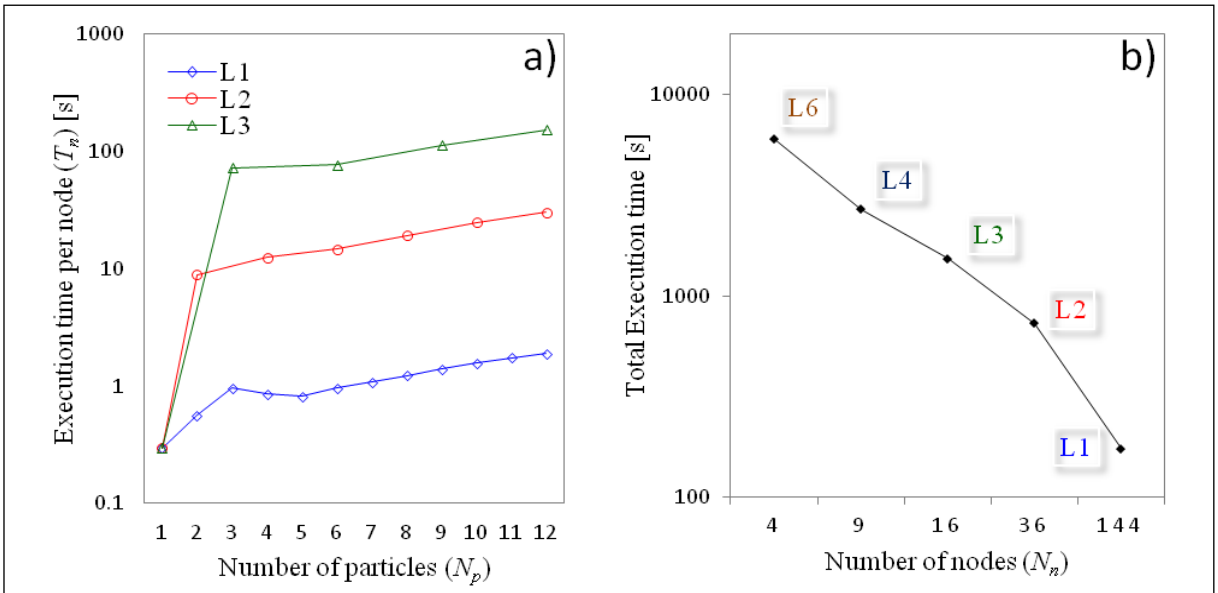

Figure 9. *a) Execution time per node, T_n, vs. the number of particles, $N_p = 1,2,\ldots,12$, for the case considered in Fig. 8, with three mapping levels, Lm, $m = 1, 2, 3$. b) Strong scalability trend for a cluster of N_p=12 particles simulated with parallel mapping levels Lm, $m = 6,4,3,2,1$, corresponding to N_n=4, 9, 16, 36, 144 nodes, respectively.*

For a more in-depth analysis of the performance of OPTIMET-3D, the examination of the *per node* execution time, T_n, is considered as shown in Fig. 9(a). This analysis clearly demonstrates that as one moves from the serial code execution corresponding to the single-sphere problem (and therefore from single-node execution) to the parallel branch of the software, one observes a steep increase in the corresponding per node execution time, T_n. In addition, this increase in T_n is considerably larger in the case of L3 scheme as compared to those of L2 and L1 levels. This is attributed to the fact that, for the cases studied here, the total simulation time for the serial case is about $T_{tot} = T_n = 0.295$s, namely, the communication costs greatly dominate over the computation time. Moreover, as the mapping level increases, the number of required nodes N_n decreases, and therefore the size of the message per communication also increases. Therefore, it is expected to observe a higher increase in T_n as m increases, as in fact Fig. 9(a) illustrates. It should also be noted that the L1 scheme was characterised by a smaller increase in T_n for an arbitrary N_p. This suggests that the L1 scheme provides the fastest and

most uniform CPU performance when compared to $Lm,\ m > 1$. Nevertheless, this is achieved at the expense of an increased N_n, which is regarded as a drawback of using only L1. Thus, OPTIMET-3D offers great flexibility in the levels of achievable parallelisation, as seen suitable by the user, based on the desired simulation and hardware availability.

6.2 Scalability Analysis

In this section, the strong scalability of the parallelised branch of OPTIMET-3D is demonstrated. For this, we consider a fixed problem size, $N_p = 12$, and measure the required computation time corresponding to increasingly larger number of nodes, N_n. Because of the particular characteristics of OPTIMET-3D's parallel mapping schemes, the number of associated processing nodes, N_n, is determined by the level of mapping applied, $Lm,\ m \geq 1$. In this test, we chose $m = \{6,4,3,2,1\}$, which resulted in N_n= {4, 9, 16, 36, 144} processes, respectively. Constrained by the per node memory limitations of the available HPC clusters (*e.g.*, each node on the *Legion* cluster can access only 4 GB of RAM), in this study we limited the number of angular harmonics to $n_{max} = 20$, thus allowing for the L6 test case. It should be noted that this relatively small value of n_{max} has a very limited influence on the overall scalability of the parallelised solver. Moreover, the use of $n_{max} = 20$ is usually well suited for cases in which the electromagnetic field is not too spatially inhomogeneous, such as clusters of large dielectric particles separated by distances of around 1/10 the size of the operating wavelength. In cases where higher precision requirements are needed, the user can use the L4 or L3 mapping levels.

The strong scalability of the parallel branch of OPTIMET-3D is clearly demonstrated by the plots in Fig. 9(b). The linear reduction in the total execution time as the order m of the parallelisation level is

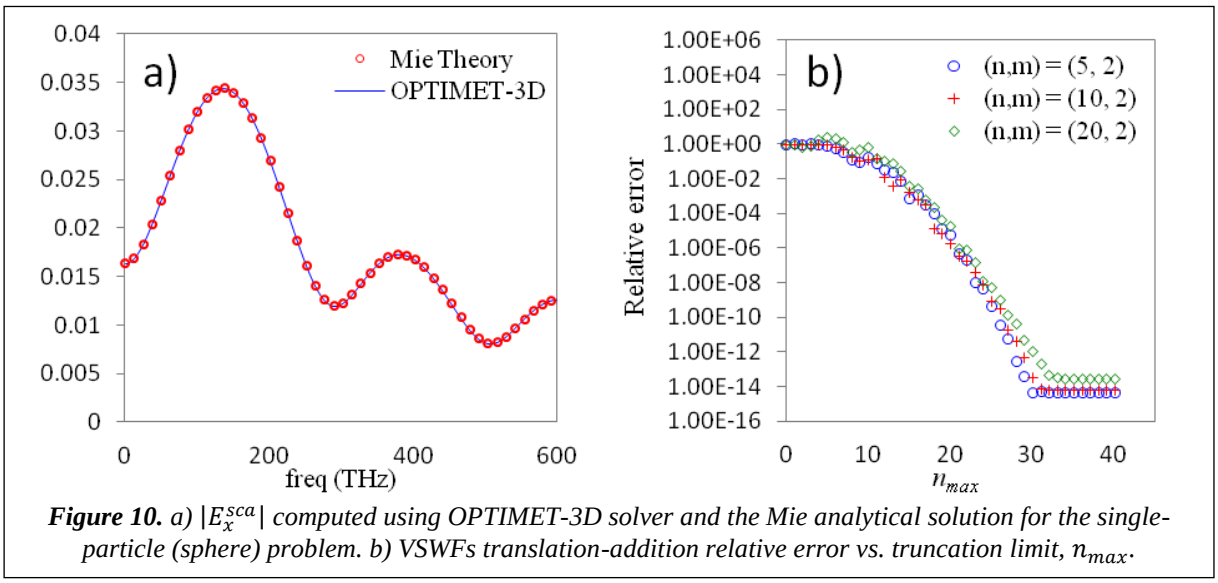

Figure 10. *a) $|E_x^{sca}|$ computed using OPTIMET-3D solver and the Mie analytical solution for the single-particle (sphere) problem. b) VSWFs translation-addition relative error vs. truncation limit, n_{max}.*

reduced (*i.e.*, number of nodes is increased) is a direct consequence of the nature of the employed parallelisation mappings, as well as the way in which the corresponding levels evenly balance out all of the additional work load and related inter-process communication. The higher mapping levels require fewer nodes, thus, they require less inter-node communication. On the other hand, the work load distributed to each node has now increased. This is clearly demonstrated when comparing the total execution time as Lm increases, where the per node computation time dominates over the communication costs. In fact, even for lower L*m*, where the contribution of inter-node communications becomes more important, the strong scalability still holds. To conclude, the OPTIMET-3D software demonstrates an excellent parallel performance, where various mapping levels can be applied with similar effectiveness, thus, allowing the user to target a desired execution time.

7. Code Validation and Practical Examples

In this section we present the results of a few tests we performed in order to validate the code implementation and give an example of a scientific problem that OPTIMET-3D can be used to investigate. Thus, we first examine the electromagnetic wave scattering from a sphere and compare analytical results based on Mie theory with those obtained using OPTIMET-3D. Then, we show the results of some numerical experiments illustrating convergence of the translated VSWFs, which are used throughout the code. Finally, we illustrate how OPTIMET-3D can be used to investigate a nano-photonics problem, namely, light scattering from a dimer and chiral clusters of silicon nano-spheres.

7.1 Single Particle Problem - Sphere

Consider a homogeneous sphere of radius $r = 0.5\,\mu$m, made of nonmagnetic, lossless and non-dispersive material with relative permittivity $\epsilon_r = 1.21$, embedded in a homogeneous medium with $\epsilon = 1$ and $\mu = \mu_r = 1$. The sphere is excited with a monochromatic electromagnetic plane wave with frequency, $\nu \leq 600$ THz. The scattered electric field, $\boldsymbol{E}^{sca}(\boldsymbol{R})$, $\boldsymbol{R} = (1, \pi, 0)$, is calculated using OPTIMET-3D and the analytical formalism based on the Mie theory [2]. The field $|E_x^{sca}|$ calculated by using these two methods is plotted in Fig. 10(a). These results clearly demonstrate the accuracy with which OPTIMET-3D can perform these field calculations.

7.2 Validation of code implementation of the Vector Translation-Addition Theorem

At the heart of the MSM algorithm is the ability to translate incoming and outgoing VSWFs, expressed in the co-ordinate system with origin in O_j, to a co-ordinate system with origin in O_l. This is achieved by using the *vector translation-addition theorem*:

$$\mathbf{M}_{mn}^{(1)}(k\boldsymbol{R}_l) = \sum_{\upsilon\mu} \left[A_{\nu\mu,mn}^{(1)}(k\boldsymbol{R}_{lj})\mathbf{M}_{\nu\mu}^{(1)}(k\boldsymbol{R}_j) + B_{\nu\mu,mn}^{(1)}(k\boldsymbol{R}_{lj})\mathbf{N}_{\nu\mu}^{(1)}(k\boldsymbol{R}_j) \right], \tag{14}$$

where $A^{(z)}(k\boldsymbol{R})$ and $B^{(z)}(k\boldsymbol{R})$, $z = 1,3$, represent the vector translation-addition coefficients [2, 4]. In order to illustrate the validity of our computer implementation of these relations, we plot in Fig. 10(b) the relative error as function of the truncation limit used in calculating the sum in Eq. (14), n_{max}, for a translation distance $R_0 = 2R_j$, $R_j = 3\,\mu$m, and $k = 10$. Note that such convergence tests are extremely useful in assessing the size of particle clusters that can be modelled with OPTIMET-3D, as well as the number of harmonics that one must include to study clusters of particles made of specific materials. This information, in turn, will be used when the `Balancer` class will be fully implemented.

7.3 Two Particles Problem – Dimer

In a more complex test, we calculated the spatial distribution of the electromagnetic field scattered by two dielectric spheres made of silicon, at both the FF and SH. This allowed us to test both the linear and non-linear branches of OPTIMET-3D. The results are plotted in Fig. 11. As expected, the field profile at the FF has a symmetric scattering pattern that suggests the interference between the incoming and scattered waves, whereas at the SH the field originates at the surface of the two spheres made of silicon. The field profiles in Fig. 11 also show the field discontinuities at the surface of the two spheres, which illustrates that the boundary conditions are properly incorporated in the code.

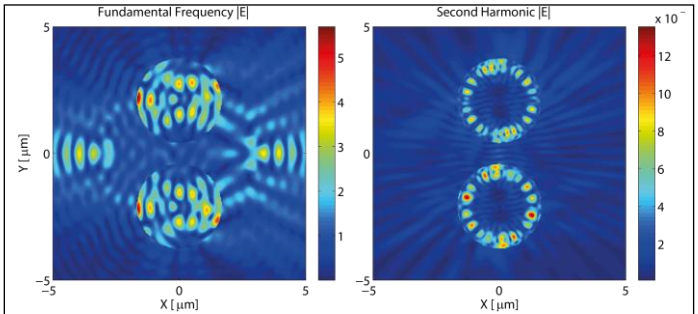

Figure 11. *Field profile at FF (left) and SH (right), respectively, generated by scattering from two silicon spheres.*

7.4 Super-Chirality from a Cluster of Dielectric Nano-Spheres

As an example of how OPTIMET-3D is used to study a problem of practical importance, we present in this section the results of a few simulations pertaining to light interaction with a chiral nano-optical structure. In particular, we demonstrate that the scattered optical field of photonic nanostructures with intrinsic chirality, which are made of silicon spheres, exhibits strong optical chirality as well as enhanced circular differential scattering. In addition, this analysis shows that using such resonant chiral nanostructures allows one to easily achieve super-chiral optical fields whose optical chirality is more than two orders of magnitude larger than that of circularly polarised plane waves.

The nano-cluster consists of silicon spheres with radius $R = 230$ nm, arranged in a chiral pattern. The cluster is excited by a circularly polarized plane wave with wavelength, $\lambda = 920$ nm, which is chosen to coincide with one of the optical resonances (TE mode) of the spheres. The optical resonances are

determined by computing the spectrum of the field enhancement at an arbitrary position near one of the spheres, as indicated in Fig. 12. The chirality of the optical field, C, can be calculated once the field distribution is known. For super-chiral fields, $|C| > 1$. Our analysis shows that the chirality of the

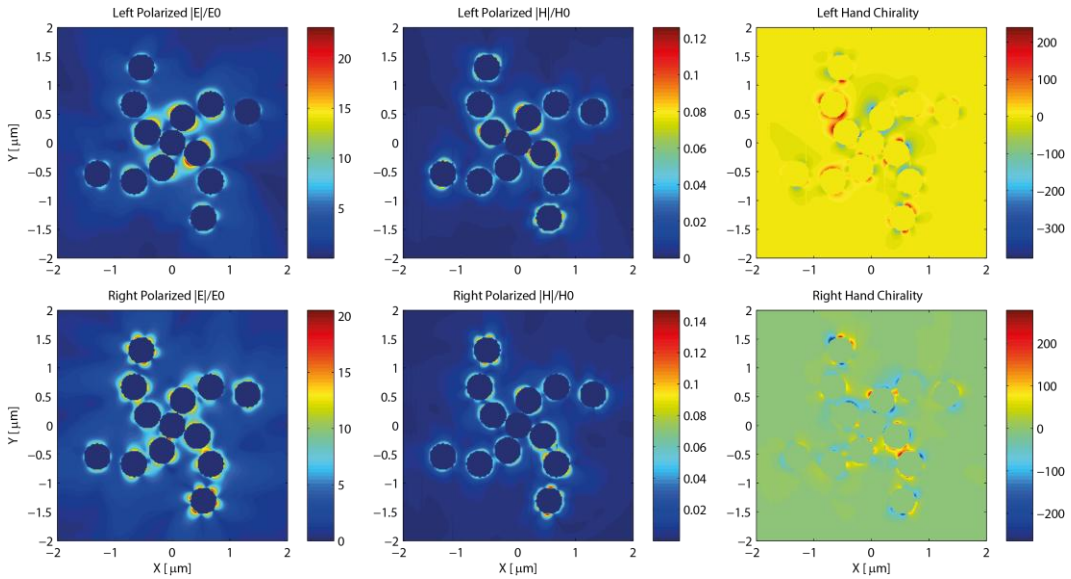

Figure 12. *Electromagnetic field distribution and optical chirality of the scattered field of a chiral nano-sphere cluster for left- (top panels) and right- (bottom panels) circularly polarised light.*

optical field is strongly enhanced at the resonance wavelength when the cluster is perpendicularly illuminated by circularly polarized plane waves, the field being highly super-chiral in large domains. In particular, more than two orders of magnitude enhancement of the chirality is observed. Importantly, the chirality of the optical near-field also indicates a strong circular differential scattering of the chiral cluster we investigated.

8. Project Impact

The main aim of this project, which has been fully accomplished, was to develop an open source HPC software to be used on UCL's HPC main system, *Legion*. Because of its portability and easy to use features, OPTIMET-3D can be easily installed and used on HPC systems with different configurations. The software was designed to model both the linear and non-linear interaction of electromagnetic waves with arbitrary distributions of 2D and 3D particles. In the 3D case one can impose periodic boundary

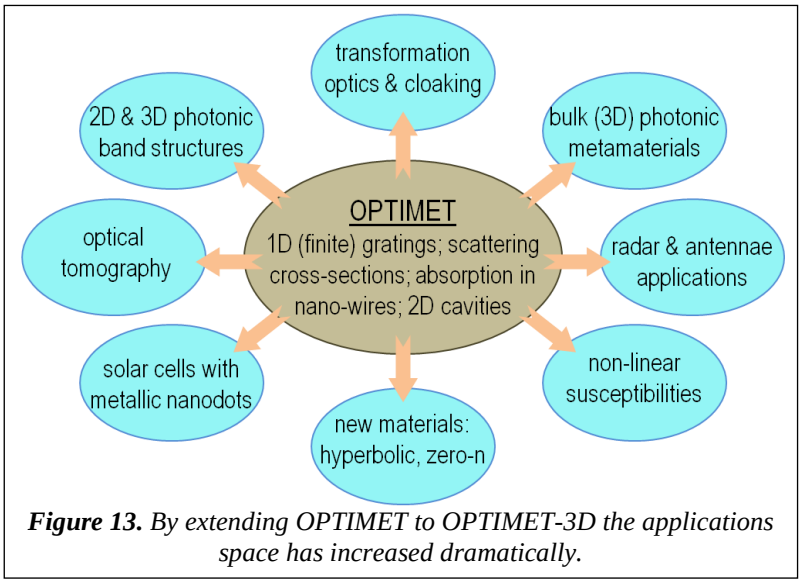

Figure 13. *By extending OPTIMET to OPTIMET-3D the applications space has increased dramatically.*

conditions, which enhances the spectrum of science and engineering problems that can be studied. Equally important, the range of materials that can be described by OPTIMET-3D covers most cases of practical interest, including, metals, dielectrics, polaritonic materials and semiconductors.

As illustrated in Fig. 13, by extending OPTIMET to 3D structures we have dramatically increased the spectrum of science and engineering problems that we can investigate. Thus, to outline just a few of its

features important for practical applications, OPTIMET-3D can now be used to investigate linear and non-linear optical properties of realistic, 3D photonic systems and devices, which are randomly or periodically structured, it can be used to compute effective linear and non-linear optical constants, such as effective permittivity and effective non-linear susceptibilities of metamaterials and it can be used to calculate the optical absorption in systems of particles. These functionalities make OPTIMET-3D extremely useful in studying a series of problems pertaining to linear and non-linear photonic and plasmonic crystals, absorption engineering (with applications to solar cells and other photovoltaic devices), transformation optics, optical tomography, colloidal chemistry and many others.

We intend to use OPTIMET-3D in a series of research projects, as part of ongoing collaborations and new ones. A brief outline of such projects is presented in what follows.

- We plan to use OPTIMET-3D to study the non-linear optical properties of non-linear plasmonic metamaterials (in collaboration with Dr Paul Warburton's Group at UCL).
- We will use OPTIMET-3D to study the absorption/emission properties of molecules placed at nanometre distance from metallic nano-particles (in collaboration with Prof Richard Osgood's Group at Columbia University). This work is particularly relevant to the design of next-generation solar cells that incorporate plasmonic materials.
- In collaboration with Prof Jeremy Baumberg and Dr Ventsislav Valev (University of Cambridge) we will use OPTIMET-3D to interpret experimental data regarding optical properties of self-assembled clusters of metallic nano-particles.
- We will use OPTIMET-3D to study multi-colour Anderson wave localisation in disordered ensembles of dielectric nano-particles (in collaboration with Prof Chee Wei Wong's Group at Columbia University).
- We will use OPTIMET-3D to study optical properties of quantum meta-materials, *a project supported by EPSRC/NSF (EP/J018473/1)* (in collaboration with Prof Shuang Zhang's Group at the University of Birmingham and Prof Xiang Zhang's Group at Berkeley University).

9. Conclusions and Future Work

In this report we have described the structure, code implementation (parallel and serial), validation tests and a few application examples of OPTIMET-3D. *This HPC software package has been developed with support from EPSRC's University distributed Computational Science and Engineering (dCSE) Programme*. OPTIMET-3D has been written and tested for validity and scalability, as illustrated in this report, with strong scalability being proven. It can be used to model a broad array of science and engineering problems, including photonic and plasmonic crystals, absorption engineering, nanoscience and nanotechnology, plasmonics, transformation optics, optical tomography and colloidal chemistry.

The HPC code has been developed for *Legion*, UCL's main HPC cluster, but has been tested on two other HPC systems, the InfraGrid and BlueGene/P clusters at the West University of Timisoara. The fully verified and tested code will be made available through the *BitBucket* website, a dedicated webpage at UCL and through the program library of Computer Physics Communications journal *via* a peer-reviewed journal article. The uni-dCSE support was for 12 months FTE divided between two people, Dr Ahmed Al-Jarro and Dr Claudiu Biris. A conference paper based on OPTIMET-3D will be presented shortly after the project has ended [6].

In order to further advance the functional capabilities of OPTIMET-3D, while building on the success of this initial project, we plan a set of future code development activities.

- We plan to port OPTIMET-3D on massively parallel architectures, including UK's HECToR and ARCHER, the next national HPC facility for academic research. For this, subsequent uni-dCSE projects, when called for, or future dCSE support will be sought.
- We will explore the portability of OPTIMET-3D to multi-GPU HPC clusters (one such cluster is available at UCL).
- We plan to make OPTIMET-3D the electromagnetic solver, which when combined with a quantum mechanical solver, will provide the unique functionality of modelling hybrid classical/quantum mechanical physical systems [13-15].
- We will implement the dynamical `Balancer` described in Sec. 5, which will help distribute among the nodes the work load in a more balanced way.

- We will implement the hybrid mapping scheme for parallelisation, which could prove to be more effective in both balancing the work load among the nodes and offering the highest flexibility in the available computing resource.
- In order to make the code easier to use, we plan to add a GUI that would allow graphical input of the simulation parameters. Note that since we use XML standards, such a GUI could be easily adapted from existing XML editors.

ACKNOWLEDGEMENT

This project was funded under the HECToR Distributed Computational Science and Engineering (CSE) Service operated by NAG Ltd. HECToR – A Research Councils UK High End Computing Service – is the UK's national supercomputing service, managed by EPSRC on behalf of the participating Research Councils. Its mission is to support capability science and engineering in UK academia. The HECToR supercomputers are managed by UoE HPCx Ltd and the CSE Support Service is provided by NAG Ltd. http://www.hector.ac.uk.

References

[1] C. F. Bohren and D. R. Huffman, *Absorption and Scattering of Light by Small Particles*, (Wiley-Interscience, 1983).

[2] M. Mishchenko, L. Travis, and A. Laci, *Scattering, Absorption and Emission of Light by Small Particles*, (Cambridge University Press 2002).

[3] M. I. Mishchenkoa, G. Videenb, V. A. Babenkoc, N. G. Khlebtsovd, and T. Wriedt, "*Comprehensive T-matrix reference database: A 2004–06 update*," J. Quant. Spectr. Rad. Trans. **106**, 304–324 (2007).

[4] B. Stout, J.-C. Auger, and J. Lafait, "*A transfer matrix approach to local field calculations in multiple scattering problems*," J. Mod. Opt. **49**, 2129–2152 (2002).

[5] C. G. Biris and N. C. Panoiu, "*Second harmonic generation in metamaterials based on homogenous centrosymmetric nanowires*," Phys. Rev. B, **81**, 195102 (2010).

[6] C. G. Biris, A. Al-Jarro, and N. C. Panoiu, "*Super-chiral Effects in Silicon Nano-sphere Clusters*," Proceedings of the 34 Progress in Electromagnetics Research (PIERS), Stockholm, Sweden, Aug. 12-15 (2013).

[7] A. Capretti, C. Forestiere, L. D. Negro, and G. Miano, "*Full-wave analytical solution of second-harmonic generation in metal nanospheres*", arXive, 2013.

[8] T. Heinz, "*Second-order nonlinear optical effects at surfaces and interfaces*," in *Nonlinear surface electromagnetic phenomena, Modern problems in condensed matter sciences*, edited by H. Ponath and G. Stegeman, pp. 353–416 (1991).

[9] M. Lax, "*Multiple scattering of waves*," Rev. Mod. Phys. **23**, 287–310 (1951).

[10] N. Stefanou and A. Modinos, "*Scattering of light from a two-dimensional array of spherical particles on a substrate*," J. Phys.: Condens. Matter **3**, 8135–8148 (1991).

[11] N. Stefanou, V. Karathanos, and A. Modinos, "*Scattering of electromagnetic waves from periodic structures*," J. Phys.: Condens. Matter **4**, 7389–7400 (1992).

[12] C. G. Biris and N. C. Panoiu, "*Nonlinear pulsed excitation of high-Q optical modes of plasmonic cavities made of metallic nanowires*," Opt. Express **18**, 17165–17179 (2010).

[13] M. Bahl, N. C. Panoiu, and R. M. Osgood, "*Optical and thermal finite-difference time-domain model for passively mode-locked surface-emitting lasers*," J. Opt. Soc. Am. B **26**, 1558-1568 (2009).

[14] H. Chen, J. M. McMahon, M. A. Ratner, and G. C. Schatz, "*Classical Electrodynamics Coupled to Quantum Mechanics for Calculation of Molecular Optical Properties: a RT-TDDFT/FDTD Approach*," J. Phys. Chem. C **114**, 14384-14392 (2010).

[15] L. Pierantoni, D. Mencarelli, and T. Rozzi, "*A New 3-D Transmission Line Matrix Scheme for the Combined Schrödinger–Maxwell Problem in the Electronic/Electromagnetic Characterization of Nanodevices,*" IEEE Trans. Microwave Theor. Tech. **56**, 654–662 (2008).